processes

MDPI

*Article*

# CFD Predictions for Mixing Times in an Elliptical Ladle Using Single- and Dual-Plug Configurations

**Rohit Tiwari [1], Bruno Girard [2], Chantal Labrecque [2], Mihaiela M. Isac [1,*] and Roderick I. L. Guthrie [1]**

[1] McGill Metals Processing Centre, McGill University, 3610 University Street, Wong Bldg. Room 2M040, Montreal, QC H3A 0C5, Canada; rohit.tiwari@mail.mcgill.ca (R.T.); roderick.guthrie@mcgill.ca (R.I.L.G.)
[2] Rio Tinto Fer et Titane, 1625 route Marie-Victorin, Sorel-Tracy, QC J3R 1M6, Canada; bruno.girard@riotinto.com (B.G.); chantal.labrecque@riotinto.com (C.L.)
* Correspondence: mihaiela.isac@mcgill.ca

**Abstract:** Argon bottom stirring is commonly practiced in secondary steelmaking processes due to its positive effects on achieving uniform temperatures and chemical compositions throughout a steel melt. It can also be used to facilitate slag metal refining reactions. The inter-mixing phenomena associated with argon gas injection through porous plugs set in the bottom and its stirring efficiency can be summarized by evaluations of 95% mixing times. This study focuses on investigating the impact of different plug positions and ratios of argon flow rates from two plugs on mixing behavior within a 110-tonne, elliptical-shaped industrial ladle. A quasi-single-phase modeling technique was employed for this purpose. The CFD findings revealed that the optimal position of the second plug is to be placed diametrically opposite the existing one at an equal mid-radius distance (R/2). An equal distribution of argon flow rates yielded the best results in terms of refractory erosion. A comparative study was conducted between single- and dual-plug-configured ladles based on flow behavior and wall shear stresses using this method. Furthermore, a transient multiphase model was developed to examine the formation of slag open eyes (SOE) for both single- and dual-plug configurations using a volume of fluid (VOF) model. The results indicated that the dual-plug configuration outperformed the current single-plug configuration.

**Keywords:** mathematical modeling; mixing time; ladle metallurgy; gas stirring; porous plug



**Citation:** Tiwari, R.; Girard, B.; Labrecque, C.; Isac, M.M.; Guthrie, R.I.L. CFD Predictions for Mixing Times in an Elliptical Ladle Using Single- and Dual-Plug Configurations. *Processes* **2023**, *11*, 1665. https://doi.org/10.3390/pr11061665

Academic Editor: Haiping Zhu

Received: 30 April 2023
Revised: 21 May 2023
Accepted: 22 May 2023
Published: 30 May 2023



## 1. Introduction

Due to the rising need for high-quality steel products, ladle metallurgy, a secondary steelmaking process, has attracted a lot of attention over time. Ladle metallurgy is practiced by adjusting a steel's composition, cleanliness, and temperature over wide ranges to meet diverse plant and customer requirements. The technique involves a series of different steps after tapping liquid steel into a teeming ladle and before sending it to the caster. These steps include de-oxidation, composition adjustment, temperature control, degassing, cleanliness adjustments, etc. Depending upon the final grade of steel, the steelmaking professional must select different operations wisely. However, all secondary steelmaking operations have one thing in common: the injection of inert gas into the steel melt using one or more porous plugs installed in the bottom brickwork of a ladle. Since argon (Ar) gas has zero solubility in steel and is inert by nature, it is frequently used for purging a melt to ensure temperature and composition homogeneity as well as to encourage reactions that lead to the refining of the steel through slag–metal interactions. Many studies have also confirmed that argon gas injection can aid in inclusion removal.

The rate of injection of argon gas varies, depending upon end requirements, i.e., inclusion removal, floating out the non-metallic inclusions, or desulphurization of steel. The argon gas bubbles become the carrying agents, taking the non-metallic inclusions toward the slag surface. For homogenization or alloy additions, an intermediate flow rate

is needed. The dissipation of the buoyant energy of the injected gas primarily causes the homogenization of bath temperature and composition via gas bubbling. On the other hand, a relatively high argon flow rate is used for desulphurization or reoxidation, for which intense mixing conditions are desired. In Figure 1, a schematic of ladle purging in a Ladle Refining Furnace (LRF) is shown [1].

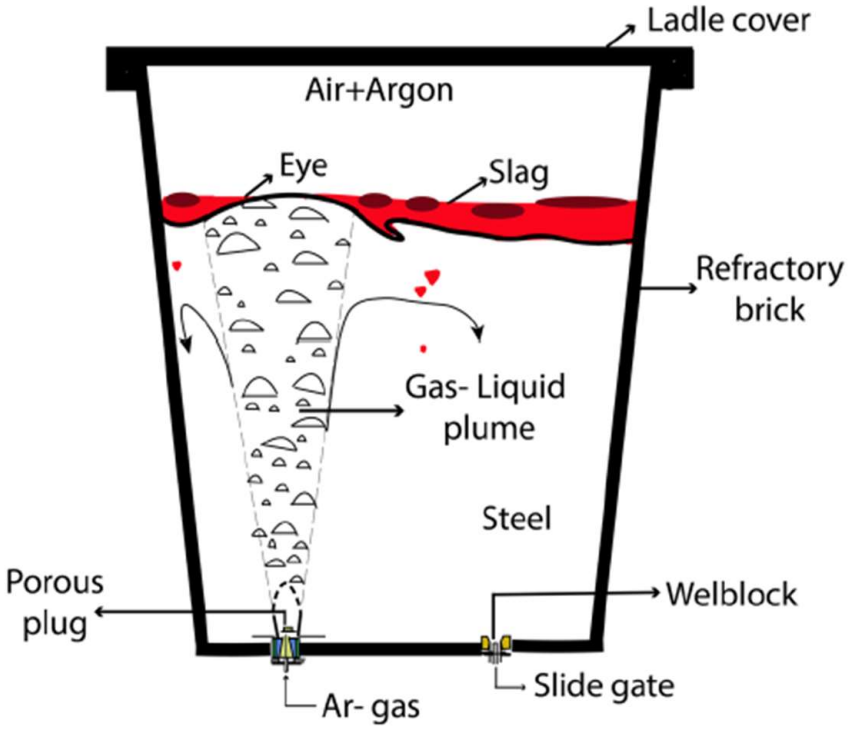


**Figure 1.** Schematic of ladle purging in a Ladle Refining Furnace (LRF) adapted from [1].

The gas rising through the melt induces a turbulent re-circulatory motion in which mass transfer-controlled processes (such as the melting of deoxidizer and alloying additions as well as their dissolution and dispersion) take place. Furthermore, as the injected gas escapes to the surroundings, the redirected bulk flow from the spout region (plume eye) pushes the slag layer radially outwards, exposing the melt surface to the ambient atmosphere. The uncovered area of the melt thus created is typically referred to as an SOE or the "slag open eye". Note that the slag eye is a potential site for reoxidation, nitrogen pick up, and slag entrainment/entrapment phenomena and hence can profoundly influence the quality of steel. Therefore, during the final stage of ladle refining and immediately before continuous casting, it is customary to practice gentle stirring (commonly termed in the industry as 'argon rinsing') to ensure a small "Slag Open Eye" (SOE) area.

Numerical studies of this gas–liquid flow phenomena in a ladle can be categorized into four methods: (a) Quasi-single-phase model, (b) Volume of Fluid (VOF) model, (c) Eulerian multiphase (E–E) model, and (d) Eulerian–Lagrangian (E–L) model. Two good review papers [2,3] have discussed all these methods in detail. In this present work, the quasi-single-phase method was used for the optimization study of the porous plug position at the bottom of the ladle. This current research opted for quasi-single-phase modeling to compare mixing times in a steel ladle with a dual-plug configuration at different plug locations and flow rates, which is a less computationally expensive method than multiphase modeling. In quasi-single-phase modeling, the gas–liquid two-phase region is considered a homogenous liquid with a slightly reduced density compared to the surrounding bulk liquid. This allows for a single set of equations of motion to be used to represent the flow in the liquid phase, where the buoyant forces resulting from gas injection are included in the momentum conservation equation in the axial or vertical

direction. To understand the state of stirring or agitation efficiency in a ladle, the concept of mixing time has been commonly used. Some previous works [4,5] have successfully validated numerically calculated mixing time using the quasi-single-phase method with their corresponding physical model. Several mathematical studies [4–9] have used mixing time in the ladle to identify the positions best suited for porous plugs to ensure rapid mixing. Several works [10–12] have been conducted to study the effect of differential gas flow rates from a dual plug. Luis et al. [10] showed that the 3:1 ratio of gas flow rate from a porous plug gives a reduced (i.e., better) mixing time compared to a 1:1 ratio of gas flow rate from the two porous plugs. In this dual-plug design, the net gas flow rate is divided into two regions, resulting in two weakened plumes compared to a single-plug system.

In addition, previous studies have explored the formation of slag open eyes using multiphase modeling techniques [13–19]. Ramasetti et al. [13] investigated the impact of top layer thickness and density on open-eye formation in a gas-stirred ladle. Mantripragada et al. [14] used the Coupled Level Set Volume of Fluid (CLSVOF) model to investigate inlet-gas-purging rate, melt height, slag layer thickness, and angular and radial positions of gas inlets affecting slag opening area. Liu et al. [15] simulated a four-phase flow consisting of bubble–steel–slag–top gas in a bottom-blown argon-stirred ladle. Results showed that at low gas flow rates, small open eyes formed and collapsed alternately, while at high gas flow rates, the size of the slag eye increased and its shape changed from circular to oval.

Apart from those studies, Liu et al. [7] have shown that a ladle with a dual-plug configuration can perform better in reducing wear on refractory linings compared to a single-plug system for an equal net flow rate of argon gas injection. The two plugs can reduce the values of interfacial velocity, reducing the potential for slag entrainment and erosion of the upper sections of the refractory wall. Similar observations are reported in some other literature [20,21].

While numerous studies have focused on simulating steel flow fields and optimizing the positions of porous plugs, these investigations have customarily been limited to cylindrical ladles. In contrast, this study aims to analyze and simulate mixing behavior within an elliptical ladle. The primary objective is to conduct a numerical investigation to determine how the arrangement of plugs and their varying flow rates would affect the mixing times in the ladle. To achieve this, a quasi-single-phase modeling approach is employed. Furthermore, this study compares the mixing behavior between a single-plug configuration and a dual-plug configuration in an argon-stirred ladle using a single-phase modeling technique for computational efficiency. Additionally, a transient multiphase model incorporating a volume of fluid (VOF) model was developed to simulate the formation of slag open eyes (SOE) in the single- and dual-plug ladle configurations.

## 2. Mathematical Modeling

Mathematical modeling was carried out using the Computational Fluid Dynamics (CFD) software ANSYS Fluent. In this present work, the simulation process was performed in two parts. In the first part, a quasi-single phase, isothermal, three-dimensional, incompressible, turbulent flow model was developed to simulate and understand flow dynamics inside an elliptical ladle and to calculate its mixing times numerically. In this case, slag and air phases in the ladle were ignored. Only the effects of argon bubbling into the ladle were considered. In the quasi-single-phase modeling, the gas–liquid two-phase region is treated as a homogeneous liquid with a slightly reduced density compared to the surrounding bulk liquid. This modeling approach ignores the interactions and exchanges between different phases and assumes constant fluid properties, such as density and viscosity, throughout the entire domain. Consequently, it fails to capture the complexity and dynamics of multiphase flows accurately, including interfacial phenomena. The objective was to numerically investigate the fluid flow behavior and mixing phenomena between a single-plug configuration and a dual-plug configuration in the argon-stirred ladle. Additionally, the effect of the different positional arrangements of an additional plug along with the existing plug is

studied in terms of mixing times. Additionally, the effect of differential gas flow rates through the two plugs was studied. As such, the relevant governing equations used in the simulation are as follows.

### 2.1. Governing Equations

#### 2.1.1. Mass Conservation Equation

$$\frac{\partial(\rho v_i)}{\partial x_j} = 0 \tag{1}$$

In Equation (1), terms $\rho$ and $v_i$ denote density (kg/m$^3$) and velocity (m/s), respectively at a point $x_j$.

#### 2.1.2. Momentum Conservation Equation

$$\frac{\partial(\rho v_j v_i)}{\partial x_j} = -\frac{\partial P}{\partial x_i} + \frac{\partial}{\partial x_i}\left\{\mu_{eff}\left(\frac{\partial v_i}{\partial x_j} + \frac{\partial v_j}{\partial x_i}\right)\right\} + \rho g \tag{2}$$

In Equation (2), the term $P$ represents pressure (Pa), $g$ is acceleration due to gravity (m·s$^{-2}$), and $\mu_{eff}$ is the effective viscosity, representing the summation of molecular viscosity and turbulent viscosity ($\mu + \mu_t$).

#### 2.1.3. Transport Equations for $k$ and $\varepsilon$ in the $k$-$\varepsilon$ Model

The kinetic energy of turbulence, $k$, is given as follows:

$$\frac{\partial(\rho v_i k)}{\partial x_i} = \frac{\partial}{\partial x_i}\left(\frac{\mu_{eff}}{\sigma_k}\cdot\frac{\partial k}{\partial x_i}\right) + G - \rho\varepsilon. \tag{3}$$

The rate of dissipation of kinetic energy, $\varepsilon$ is given as follows:

$$\frac{\partial(\rho v_i \varepsilon)}{\partial x_i} = \frac{\partial}{\partial x_i}\left(\frac{\mu_{eff}}{\sigma_\varepsilon}\cdot\frac{\partial \varepsilon}{\partial x_i}\right) + \frac{\varepsilon}{k}(C_1 G - C_2\rho\varepsilon), \tag{4}$$

where $C_1$, $C_2$, $\sigma_k$, and $\sigma_\varepsilon$ are empirical constants, whose values are 1.38, 1.92, 1.0, and 1.3, respectively. Moreover, $G$ represents the generation of kinetic energy of turbulence due to mean velocity gradients.

#### 2.1.4. Species Transport Equation

Once the flow fields have converged during simulation, the transient state is switched on for the species transport equation to visualize mass flow rate within the domain.

$$\frac{\partial(\rho C)}{\partial t} + \frac{\partial(\rho v_i C)}{\partial x_i} = \frac{\partial}{\partial x_i}\left\{\rho\Gamma_{eff}\frac{\partial C}{\partial x_i}\right\} \tag{5}$$

In Equation (5), $\Gamma_{eff}$ is the effective mass diffusion coefficient given by $\Gamma_{eff} = \frac{\mu}{S_c} + \frac{\mu_t}{S_{c,t}}$. $S_c$ and $S_{c,t}$ are the laminar and turbulent Schmidt numbers, respectively.

In the second part of the simulation, a transient, isothermal, multiphase phase (steel–slag–argon–air) model was developed. The volume of fluid (VOF) modeling technique was used to investigate slag open eye (SOE) formation. To conduct this simulation, the mass and momentum equations were solved as shown in Equations (1) and (2), respectively. Additionally, the k-ε model was used to incorporate turbulence phenomena, as shown in Equations (3) and (4). It is important to note that the transient term was added to all four equations to account for the system's transient behavior.

2.1.5. Volume of Fluid Model

The VOF method is widely used for simulating multiphase flows. It assumes incompressible fluid phases with no mass transfer between them. The VOF method tracks the interface between phases with a sharp boundary assumption, facilitating clear interface location tracking during the simulation. However, this assumption can lead to inaccuracies in capturing small-scale features or sharp gradients at the interface. In this work, it was used to track the liquid steel/slag/air interface behavior. The finite volume equation of the VOF model can be written in the following form:

$$\frac{1}{\rho_q}\left[\frac{\partial}{\partial t}(\alpha_q\rho_q) + \nabla\cdot(\alpha_q\rho_q\rho v_q) = S_{\alpha q} + \sum_{p=1}^{n}(\dot{m_{pq}} + \dot{m_{qp}})\right], \tag{6}$$

where $\dot{m_{pq}}$ and $m_{qp}$ represent the mass transfer from phase $p$ to phase $q$ and $q$ to $p$, respectively, in unit time and volume; $\alpha_q$ is the volume fraction of phase $q$; $\rho_q$ is the density of phase $q$; $S_{\alpha q}$ is a source term (=0). When the volume fractions are summed, the following equation must be satisfied:

$$\sum_{q=1}^{n}\alpha_q = 1. \tag{7}$$

*2.2. Characteristics of Gas-Liquid Plume*

In quasi-single-phase modeling, the gas–liquid mixture is modeled as a homogeneous fluid. This region is referred to as a plume; the volume fraction of gas inside the plume and the dimension of the plume region play a significant role in modeling. They are predicted with experimental results or equations available in the literature. The volume fraction of gas is estimated from the principle of volume continuity using the average rise velocity of the gas–liquid mixture and plume dimensions. Assuming a no-slip condition for this current study average gas volume fraction is given as follows:

$$\alpha_g = \frac{Q}{\pi {r^2}_{av,p} U_p}, \tag{8}$$

where $r_{av,p}$ is the average velocity of plume, and $U_p$ is plume rising velocity; Sahai and Guthrie [22] provided the following equation to calculate plume rising velocity:

$$U_p = K\frac{Q^{1/3}\,L^{1/4}}{R^{1/3}}. \tag{9}$$

Using gas volume fraction value, density of the plume can be estimated as follows:

$$\rho = \alpha_g\rho_g + (1-\alpha_g)\rho_l. \tag{10}$$

Similarly, Goldschmit and Owen [23] have estimated top surface radius of plume for a ladle with height, H containing liquid steel as $r_p = 1.5\,b$, where b is radius of plume in which gas fraction is half of centerline gas fraction, given by the following:

$$b = 0.28\,(z + H_o\,)^{7/12} * \left({Q_1}^2/g\right)^{1/12}, \tag{11}$$

where value of $H_o$ is given by the following:

$$H_o = 4.5 * {d_o}^{\frac{1}{2}} * \left({Q_0}^2/g\right)^{1/10}, \tag{12}$$

where $Q_0$ is equivalent to gas flow rate a bottom ($z$ = 0) at steel melting temperature. It is expressed as follows:

$$Q_0 = Q_g * \frac{T_L}{T_g}\frac{P_{atm}/\rho_{Lg}}{P_{atm}/\rho_{Lg} + (H-z)}, \tag{13}$$

and $Q_1$ is the equivalent gas flow rate a top ($z$ = $H$) at steel melting temperature.

### 2.3. Geometry and Mesh Setup

The geometry of an elliptical ladle operating in an industrial set-up was developed using ANSYS SpaceClaim software. Figure 2 shows the three-dimensional geometry of the elliptical ladle. For the quasi-single-phase simulation, the air region and slag layer were ignored, and the gas–liquid plume region was introduced to incorporate the effect of argon bubbling. Plume dimension calculations are discussed in the previous section. The constructed geometry was then exported to the ANSYS Meshing tool, in which a tetrahedral mesh was generated. Figure 2a presents the geometry created for the ladle with a single plug, and Figure 2b presents a dual-plug configuration. The generated mesh for the ladle with a single plug contained 217,812 nodes and 136,267 elements. Similarly, the mesh of a ladle with a dual plug had 589,903 nodes and 363,293 elements. The geometrical parameters of the ladle for the quasi-single-phase modeling are shown in Table 1.

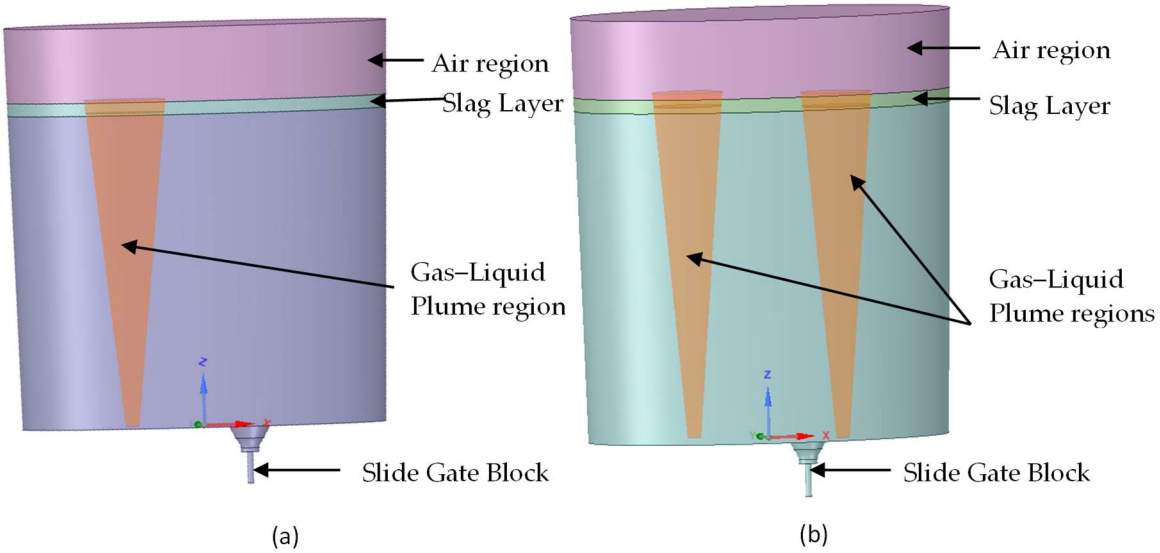


**Figure 2.** Geometry created in ANSYS SpaceClaim for (**a**) single-plug and (**b**) dual-plug configuration.

**Table 1.** Geometrical parameters of the ladle used in quasi-single-phase modeling.

| Calculation Parameter | Parameter Value | |
|---|---|---|
| | **Single-Plug Configuration** | **Dual-Plug Configuration** |
| Major axis of top surface | 1.56 m | 1.56 m |
| Minor axis of top surface | 1.16 m | 1.16 m |
| Major axis of bottom surface | 1.50 m | 1.50 m |
| Minor axis of bottom surface | 1.10 m | 1.10 m |
| Height of ladle | 2.67 m | 2.67 m |
| Plug diameter | 0.11 m | 0.11 m |
| Plume top diameter | 0.68 m | 0.60 m |
| Gas flow rate | 10 $m^3$/h | 5 $m^3$/h |

For the VOF multiphase model, all four phases (liquid steel, slag, argon, and air) were considered. The same geometries and meshes were used, as shown in Figure 2, after ignoring the plume region. The height of the air region was considered as 609 mm, and the slag layer thickness was kept at 106 mm as per the industrial setup. The details of material properties used in the mathematical model are shown in Table 2. To replicate the actual plant process, the density of argon gas is taken, corresponding to a temperature around 1100 °C [24].

**Table 2.** Material property used in VOF multiphase modeling.

| Material | Density (Kg/m$^3$) | Viscosity (Pa.s) |
|---|---|---|
| Liquid Steel | 7000 | 0.0056 |
| Slag | 3500 | 0.06 |
| Argon | 0.317 | $2.12 \times 10^{-5}$ |
| Air | 1.225 | $1.79 \times 10^{-5}$ |

## 3. Results and Discussion

### *3.1. Effect of Plug Position on Mixing Behavior*

To investigate the impact of plug position on mixing behavior, six distinct cases were identified. To create these scenarios, it was necessary to determine the location of the second plug with reference to the existing one. However, because the geometry was elliptical, direct calculation of the second position using Cartesian coordinates was not feasible. To overcome this issue, the positions were first converted to polar form ($r$, $\theta$) with the following equation:

$$r = \frac{a * b}{\sqrt{b^2 \cos^2 \theta + a^2 \sin^2 \theta}}. \quad (14)$$

In Equation (14), $r$ represents the radial distance, and $\theta$ represents the angle formed with the major axis. The major and minor axes are denoted by $a$ and $b$, respectively. Based on calculations, the existing plug was located at an angle of 38.2 degrees, at a half radius from the center of the ellipse. Using this as a reference point, six additional positions were identified at angles of 60, 120, and 180 degrees from the reference point and at distances of 0.5 and 0.75 times the radius from the center. The calculated positions are summarized in Table 3, while the locations of the plugs at the bottom of the ladle are illustrated in Figure 3. In Figure 3, Point 0 represents the location of the existing plug and Points 1–6 denote different proposed positions for the second plug. The corresponding cases selected for questioning are presented in Table 4.

**Table 3.** Different plug positions are used for modeling.

| Point | Radial Length (r) | Length Factor | Angle | X Position | Y Position |
|---|---|---|---|---|---|
| 0 | 1299 | 0.5 r | (38.2)° | −515 | 405 |
| 1 | 1416 | 0.5 r | (38.2 + 60)° | −657 | −263 |
| 2 | 1103 | 0.5 r | (38.2 + 120)° | −79 | −546 |
| 3 | 1299 | 0.5 r | (38.2 + 180)° | 515 | −405 |
| 4 | 1416 | 0.75 r | (38.2 + 60)° | −986 | −394 |
| 5 | 1103 | 0.75 r | (38.2 + 120)° | −118 | −819 |
| 6 | 1299 | 0.75 r | (38.2 + 180)° | −772 | −607 |

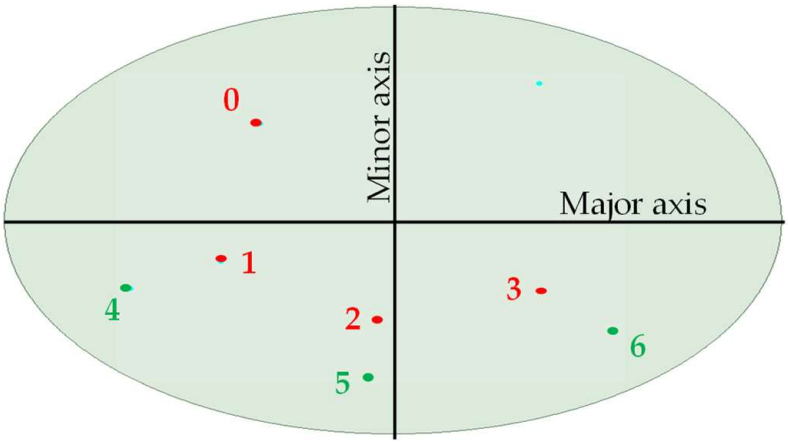


**Figure 3.** Porous plug location at the bottom of ladle. Point 0 is position of existing plug and points 1–6 are proposed plug positions.

**Table 4.** Selected cases for modeling.

| **Two Plug Placements; Cases 1–6** | |
|---|---|
| Case 1 | Point 0 + Point 1 |
| Case 2 | Point 0 + Point 2 |
| Case 3 | Point 0 + Point 3 |
| Case 4 | Point 0 + Point 4 |
| Case 5 | Point 0 + Point 5 |
| Case 6 | Point 0 + Point 6 |

Mixing times were numerically calculated for these six proposed cases to identify the best-suited position for the second plug with respect to the existing one. For this current study, mixing time was defined as the time required for all elements of the fluid to attain a 95% degree of homogenization in molten steel. To simulate alloy additions to liquid steel, the tracer (potassium chloride) is released at the point located in a straight line with the existing purging plug 0.1 m below the surface. The concentration of the tracer is checked with time at six different locations. The tracer injection point and tracker positions to calculate the mixing time in the ladle are shown in Figure 4, and their corresponding locations are given in Table 5.

**Table 5.** Coordinates of tracker positions and injection points (in mm).

| **Point** | **X** | **Y** | **Z** |
|---|---|---|---|
| Point 1 | 749 | 549 | 667 |
| Point 2 | 749 | 549 | 1334 |
| Point 3 | 749 | 549 | 2001 |
| Point 4 | −749 | 549 | 667 |
| Point 5 | −749 | 549 | 1334 |
| Point 6 | −749 | 549 | 2001 |
| Point 7 | −515 | 405 | 2568 |

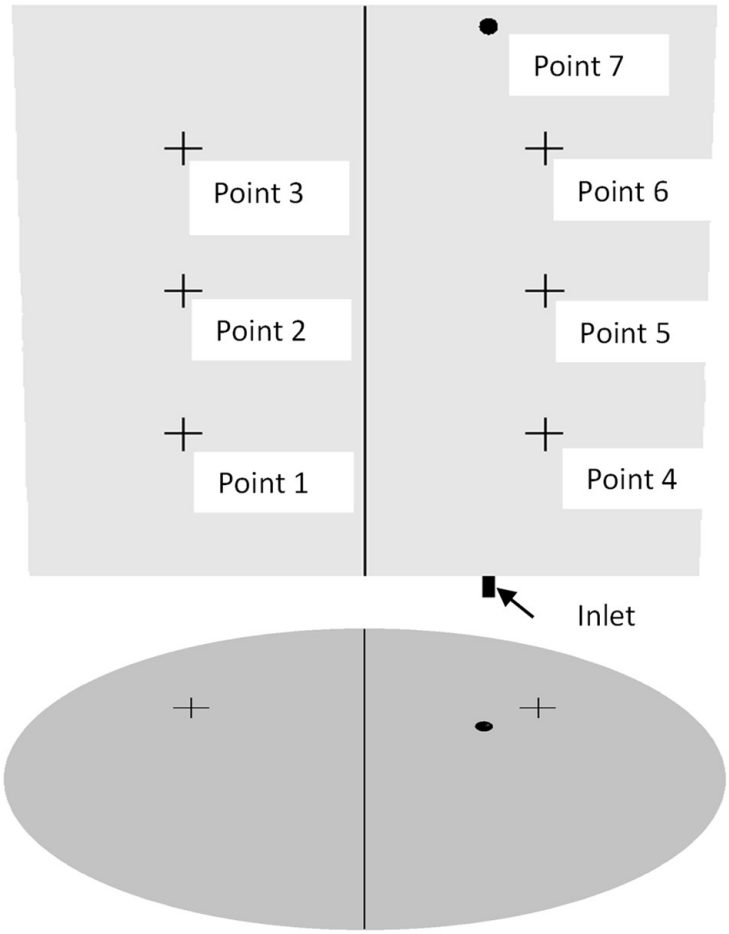


**Figure 4.** Side view (up) and top view (down) of tracker positions (1–6) and Injection Point (7).

Figure 5 shows the tracer concentration curves at various monitoring points for all the cases studied: Cases 1, 2, 3, 4, 5, and 6 are shown. Additionally, Figure 6 shows the overall mixing times for each case. It was determined that Case 3 (i.e., dual-plug configuration with plugs placed diametrically opposite each other, at half radius) provided the shortest mixing time, although Case 2 was a very close second.

Figure 7 shows tracer iso-concentration and colored contours at different times for Case 3. The colored contours are plotted on a vertical plane passing through the center of a ladle and both purging plugs (plane A, Figure 8). As shown in Figure 4, the tracer is injected at point 7, at the top surface slightly to the left of the plume (let us say plume 1). Figure 7 shows the tracer patterns at different instants of time: initially, the tracer flows around plume 1 following a recirculatory flow pattern. With increasing time, the tracer diffuses, spreading out between plume 1 and the ladle sidewall, while the tracer concentration begins to develop around the second plume. At t = 124 s, the ladle is predicted to have reached the 95% mixing criteria along the vertical plane A. It can be observed that the tracer mixing patterns follow recirculatory trends before achieving this well-mixed condition along plane A.

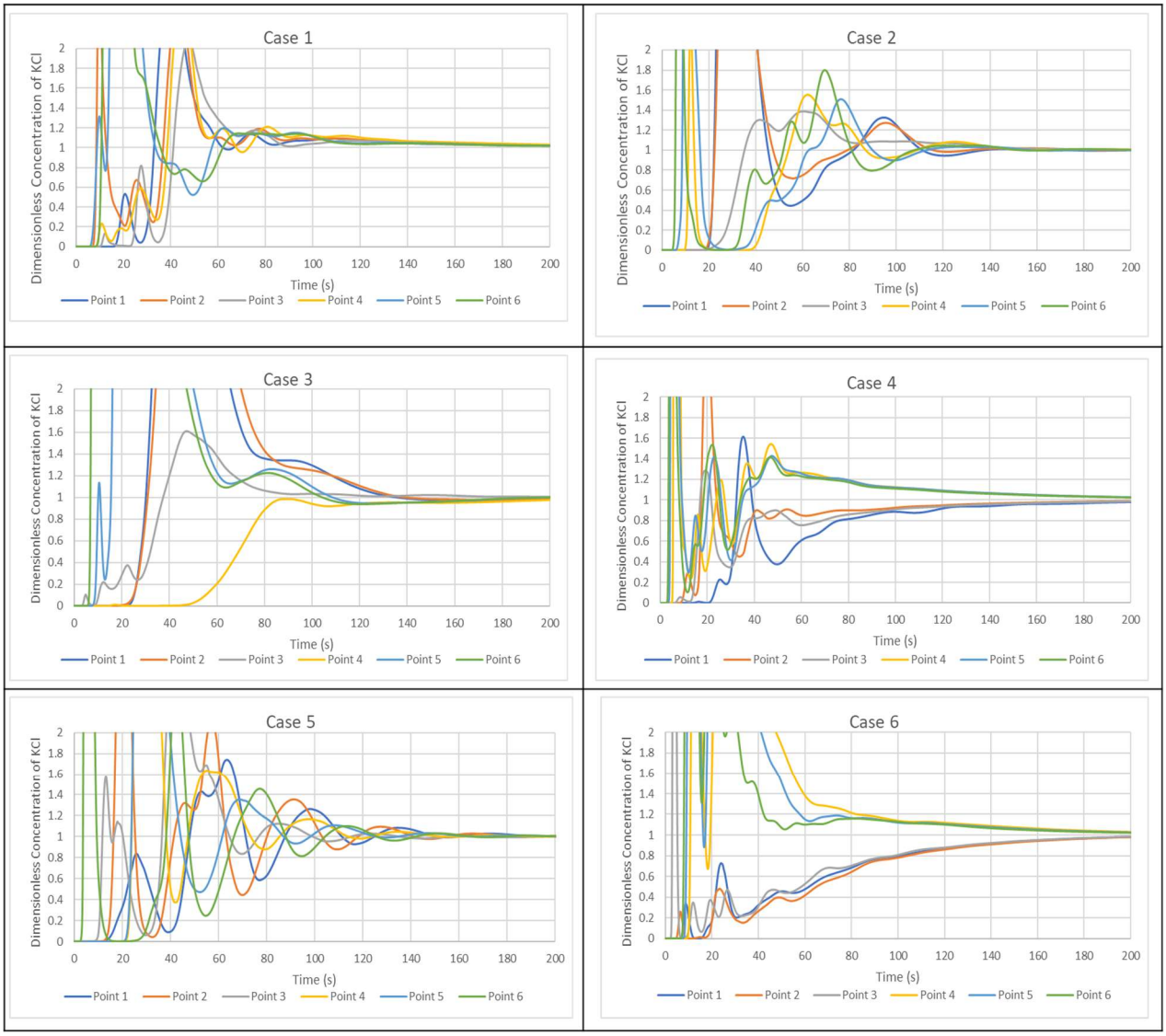


**Figure 5.** Tracer concentration curves for Cases 1, 2, 3, 4, 5, and 6 for six locations selected within the ladle.

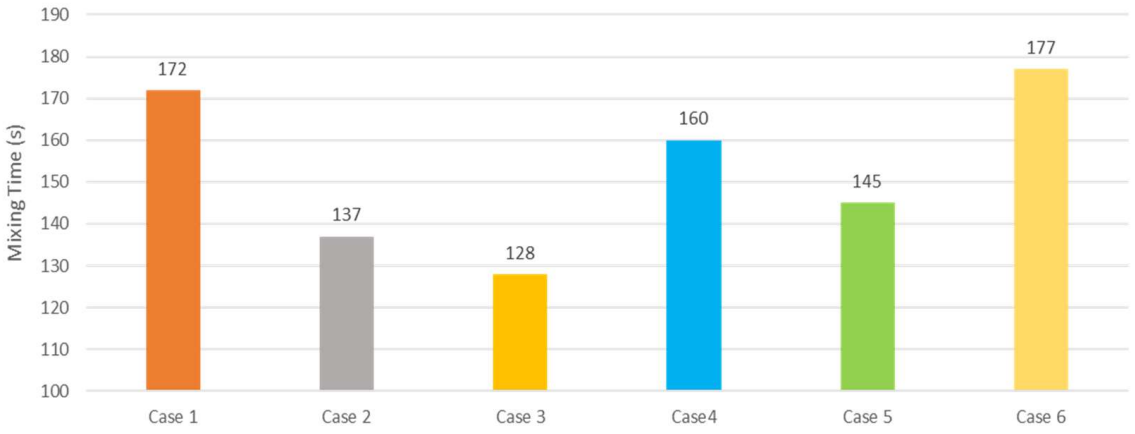


**Figure 6.** Predicted mixing for the proposed cases.

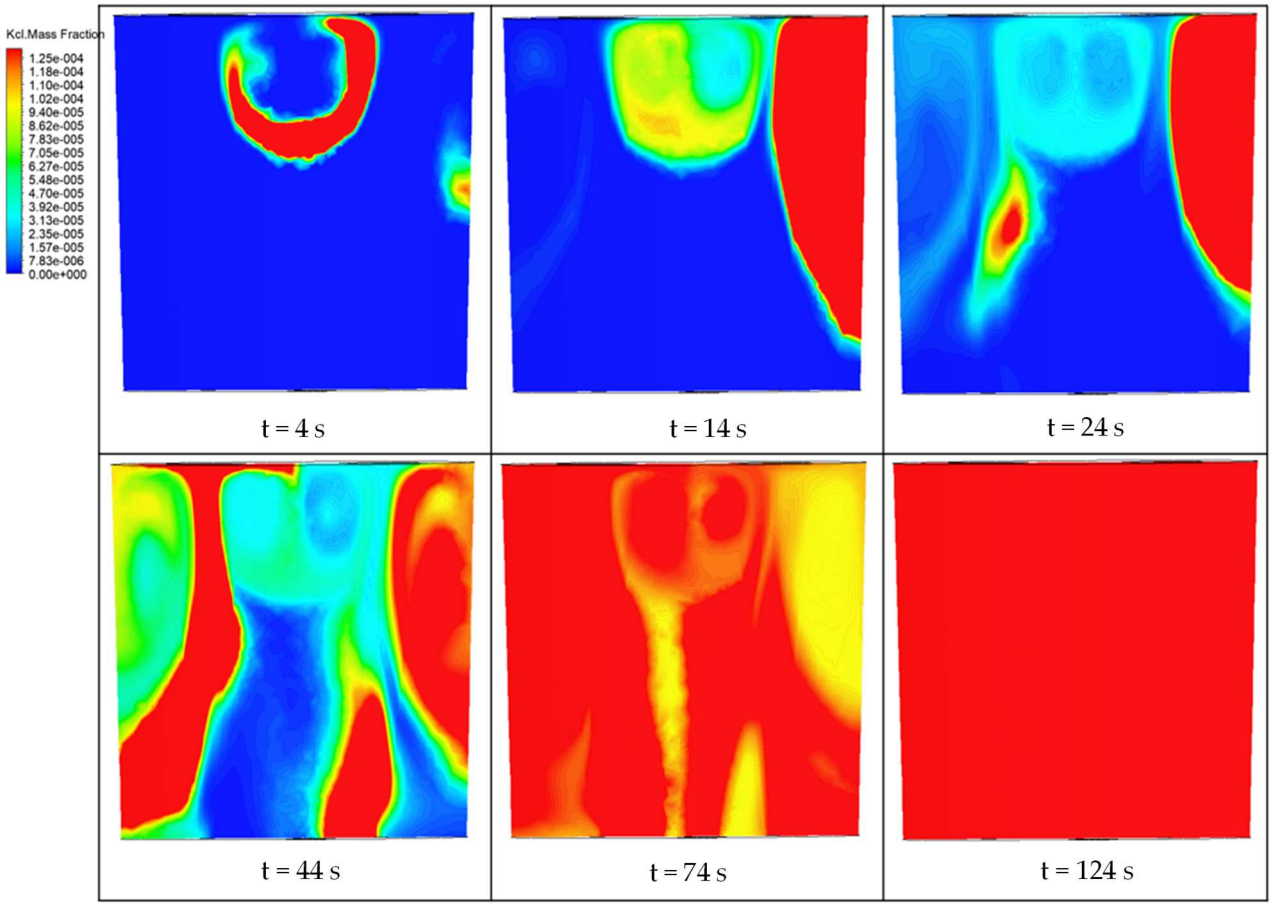


**Figure 7.** Tracer iso-concentration contours at different times from t = 4 s to t = 124 s for vertical plane A.

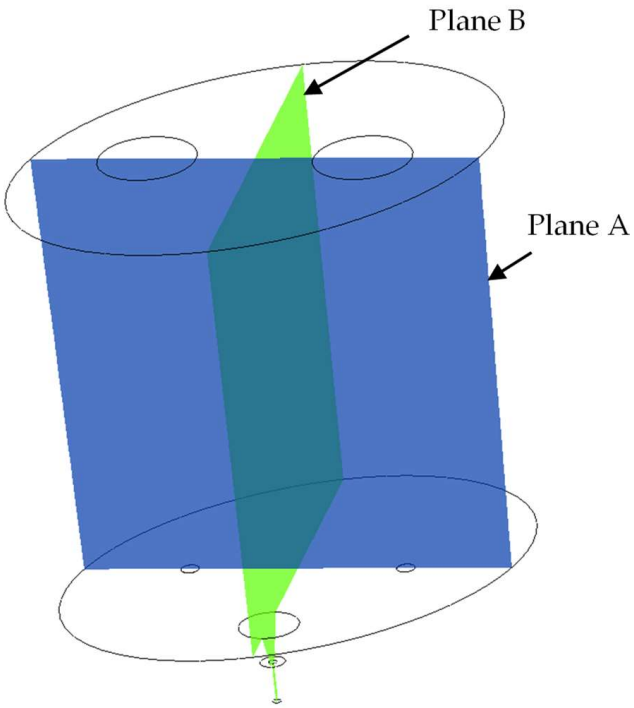


**Figure 8.** Schematic showing position of analysis plane.

### *3.2. Effect of Different Flow Rates from Plugs on Mixing Behavior*

To evaluate the impact of different plug flow rates on mixing behavior, three separate cases were devised by distributing argon in varying ratios while maintaining the same total flow rate of argon. As depicted in Table 6, for Case 7, the argon flow rate was evenly divided between both inlets, resulting in a flow rate of 5 $m^3$/h from each inlet. For Case 8, the argon flow rate was distributed in a 3:1 ratio, with a flow rate of 7.5 $m^3$/h from inlet 1 and 2.5 $m^3$/h from inlet 2, resulting in a total flow rate of 10 $m^3$/h. Similarly, for Case 9, the flow rate was distributed in a 2:1 ratio, with flow rates of 6.7 and 3.3 $m^3$/h, respectively. Based on these flow rates, plume radius and density were calculated, and mixing time was determined using the method described in the previous sections. The calculated mixing times for all cases are presented in Table 6, below. There, it is important to note that the position of the second plug was situated diametrically opposite to the existing plug at an equal radial distance.

**Table 6.** Mixing time comparison for different plug flow rates.

| | Argon Distribution | Plug | Argon Flow Rate ($m^3$/h) | Plume Radius (mm) | Plume Density (kg/$m^3$) | Mixing Time (s) |
|---|---|---|---|---|---|---|
| Case 7 | 1:1 | Plug 1 | 5.0 | 300 | 6396 | 128 |
| | | Plug 2 | 5.0 | 300 | 6396 | |
| Case 8 | 3:1 | Plug 1 | 7.5 | 323 | 6302 | 120 |
| | | Plug 2 | 2.5 | 265 | 6531 | |
| Case 9 | 2:1 | Plug 1 | 6.7 | 316 | 6330 | 133 |
| | | Plug 2 | 3.3 | 279 | 6479 | |

The results of this exercise showed that Case 8 (3:1) had the shortest mixing time of the three studied. However, it is crucial to also consider other significant variables, such as the lining life in the inevitable presence of refractory lining wear. In this regard, Figure 9 illustrates a comparative plot of hydrodynamic wall shear stresses generated for the three cases. It can be observed that for the same total argon injection rate, Case 7 has a much lower detrimental effect on the wall's erosion than the other two cases.

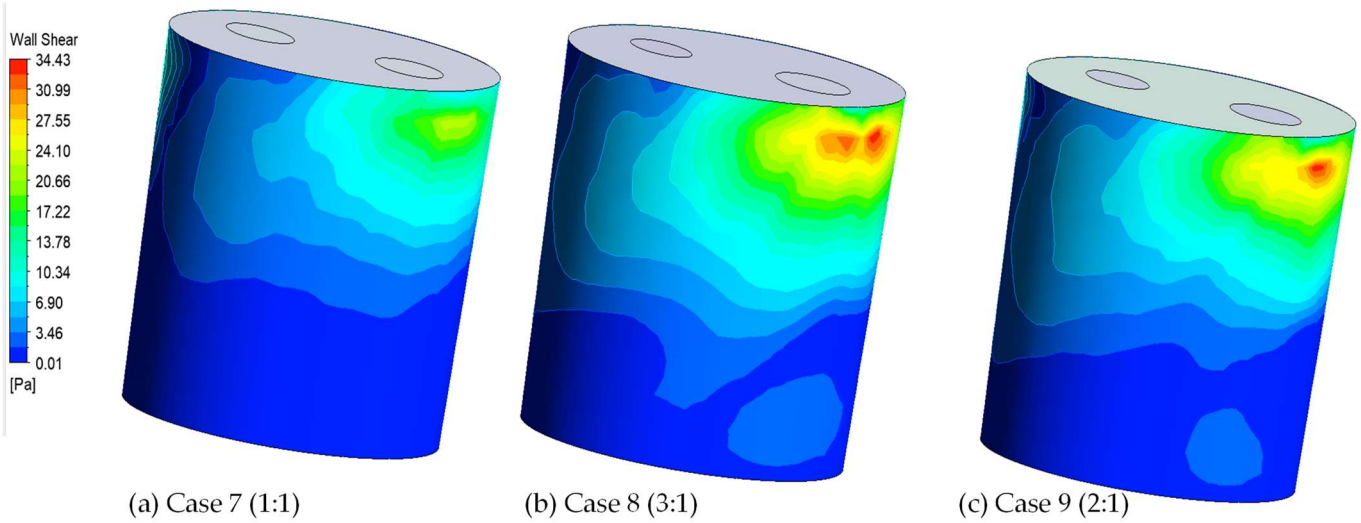


**Figure 9.** Predicted wall shears for (**a**) Case 7, (**b**) Case 8, and (**c**) Case 9.

### *3.3. Comparison of Dual-Plug with single-Plug Configuration*

Figure 10 depicts the flow patterns for the single-plug and dual-plug systems, with the velocity vector plotted on a vertical plane passing through the center of the plug and the center of the ladle (plane A in Figure 8). In the case of a single-plug configuration, two typical recirculation fluid flow patterns can be observed between the plume region and the ladle wall generated by argon injection. The size of the recirculation loop depends on the radial distance between the plug and the ladle sidewall. The recirculation flow can be characterized by an upward flow driven by injected gas, which then turns horizontally towards the sidewall in the vicinity of the free surface and, finally, into a downward flow along the sidewall. It should be noted that the plume shape is not strictly vertical conical; it is slightly tilted towards the nearest wall with increasing height in the ladle. In contrast, the flow profile for a dual-plug arrangement exhibits an additional recirculation loop between two plumes, along with two large recirculations between the plume and ladle wall. Since the gas flow rate is the same in both plugs, the flow pattern is nearly symmetrical. These figures show that the predicted results align well with the theoretical understanding of plume formation during argon injection into a ladle [7]. Due to gas injection, the gas–liquid region of both plumes expands laterally with increasing liquid height, causing the plume to split into two primary streams. Additionally, both plume shapes are slightly tilted toward the nearest ladle wall.

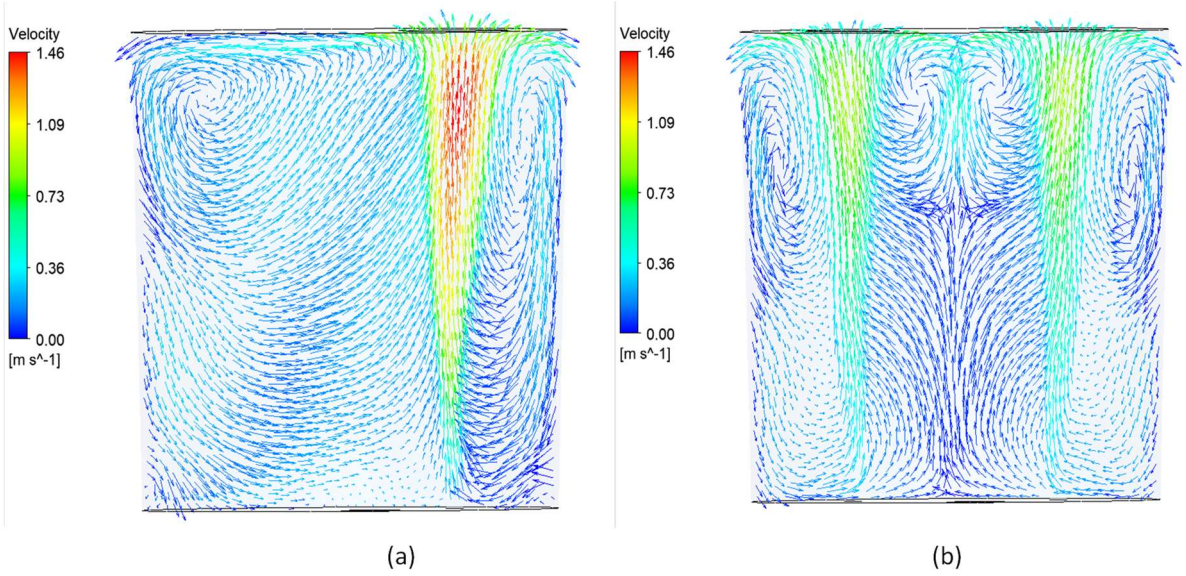


**Figure 10.** Predicted velocity profile inside ladle at plane A for (**a**) single-plug configuration and (**b**) dual-plug configuration (Case 3).

In addition to flow patterns, mixing times were also compared for the two cases. For the single-plug system, the calculated mixing time was 136 s, whereas, for the dual-plug configuration (Case 3), the mixing time was 128 s. Figure 11 shows a comparative plot of the hydrodynamic wall shear stress generated by a single-plug system with those for a dual-plug configuration (Case 3). It can be observed that the dual-plug system has a significantly lower detrimental effect on the wall's erosion compared to the single-plug system, despite having the same total argon injection rate. The maximum intensity of wall shear stress in the dual-plug system is approximately two-thirds of that observed in the single-plug system. In a single-plug configuration, higher wall shear stress can lead to accelerated erosion of the refractory material, resulting in reduced service life of the lining and increased maintenance costs.

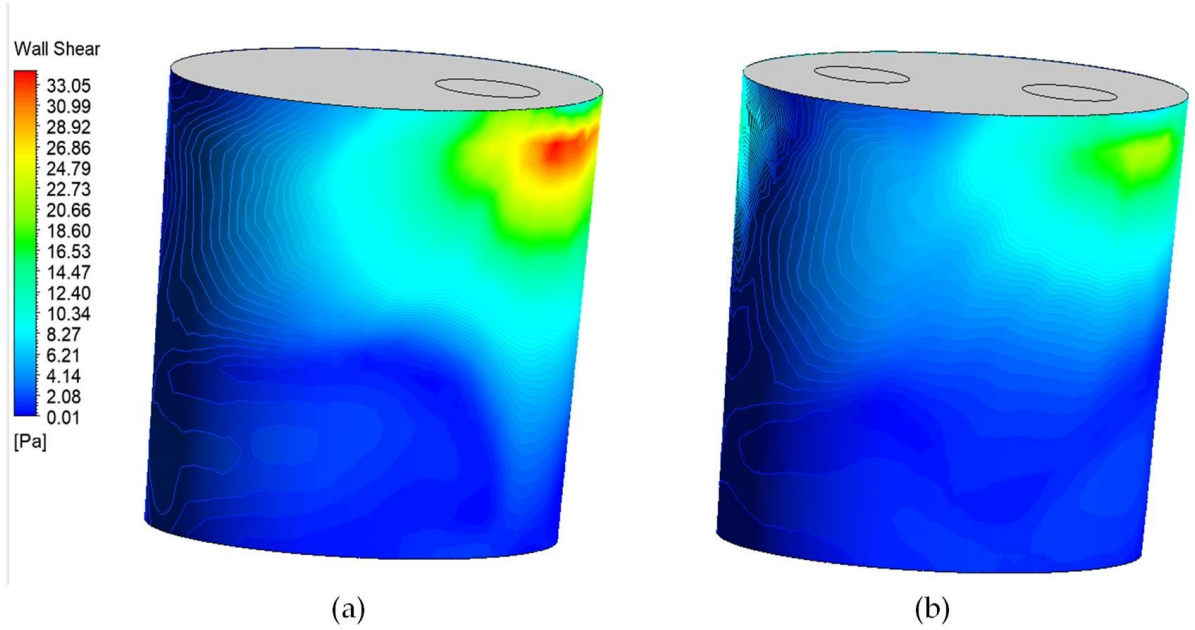


**Figure 11.** Predicted wall shear for (**a**) single-plug and (**b**) dual-plug configurations (Case 3).

The cleanliness of steel is significantly impacted by the size of the slag open eye (SOE) area, which determines the amount of liquid metal exposed to the surrounding atmosphere. This exposure can lead to increased oxidation and nitrogen absorption by the steel. Figure 12 compares the formation of SOE in single-plug- and dual-plug-configured ladles. The contour plot in Figure 12 depicts the volume fraction of liquid steel at the air/slag interface after the ladle purging process reaches a steady state. The red color represents the highest steel fraction. In the single-plug system, the argon flow rate was 10 $m^3$/h, while in the dual-plug system, the total argon flow rate was equal to the single-plug system but equally distributed between both plugs. The SOE area was found to be larger in the single-plug configuration, indicating higher slag entrainment in liquid steel than in the dual-plug system, as the impact of upward liquid steel driven by rising bubbles breaking up the slag layer is more intensive for the single-plug system.

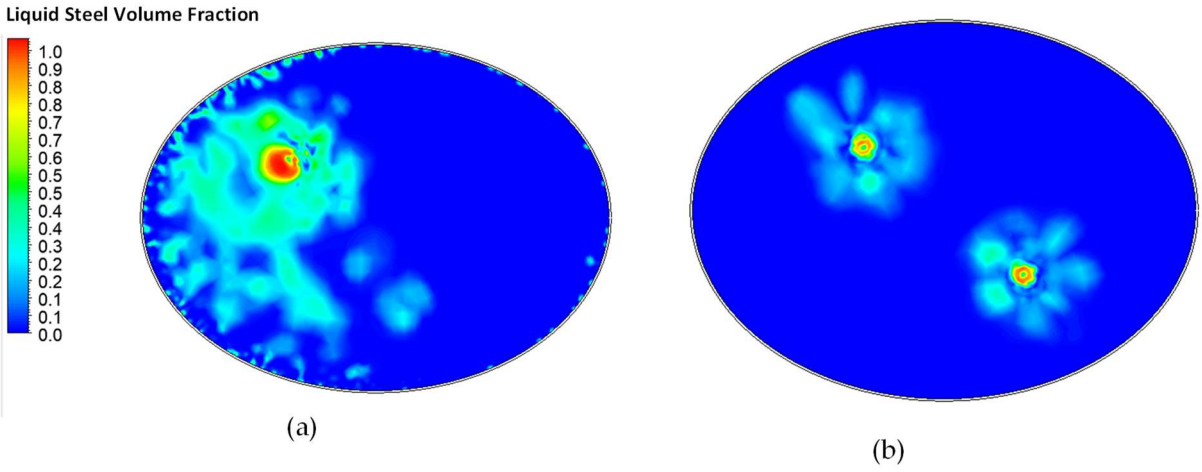


**Figure 12.** Predicted "SOE" at air–slag interface for (**a**) single-plug and (**b**) dual-plug configurations (Case 3).

Figure 13 shows the liquid steel profile (with volume fraction, $\alpha$ = 0.7) at the air and slag region for both configurations. It should be noted that the steel surface is covered by a thin layer of slag, which is disrupted by argon gas bubbles intermittently. This results in the

formation of a standing wave at the interface of slag and steel. The upwelling flow in the gas plume causes the configuration of the molten steel surface to be displayed as a spout peak in Figure 13. The use of two plugs at symmetrical locations reduces the height of the spout peak. However, the interaction between the two rising plumes on the surface makes the wave formation more complicated than for the single-plug case. Further research is necessary to assess interface wave formation on slag emulsification.

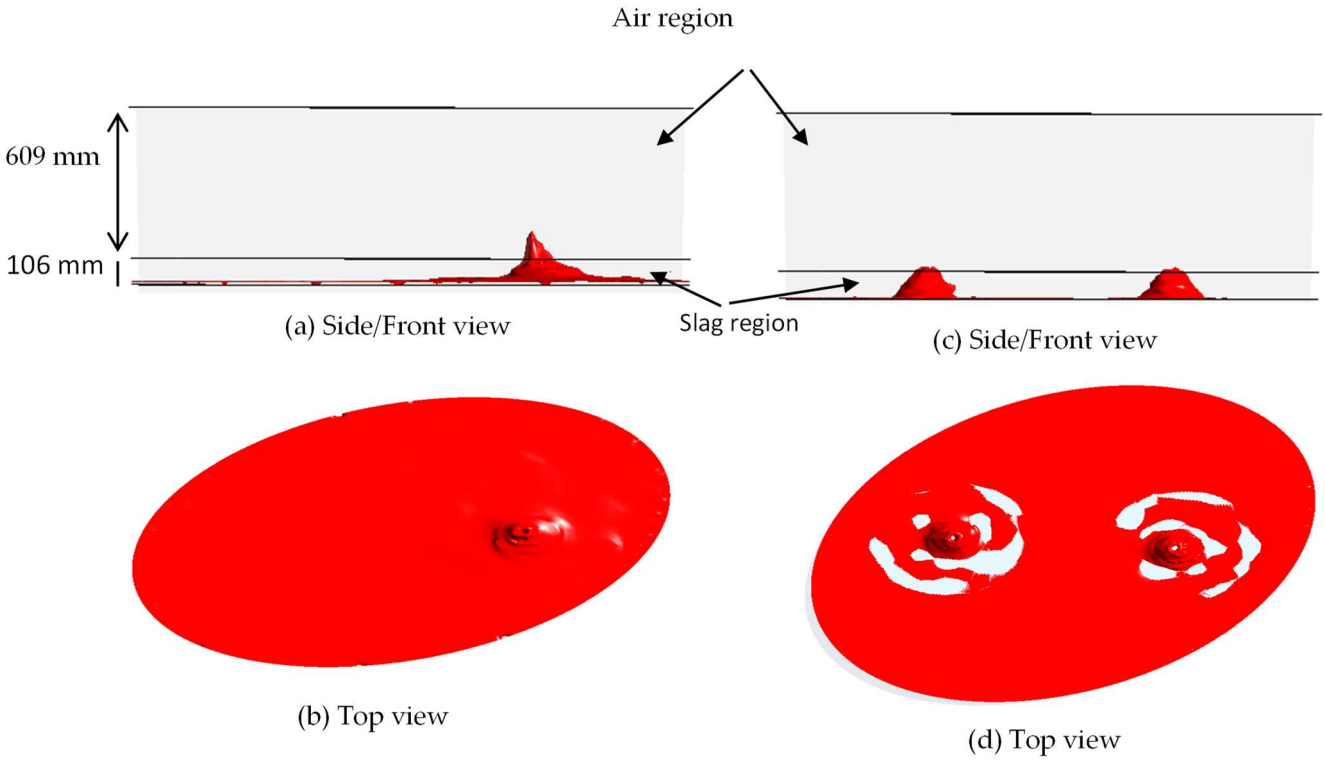


**Figure 13.** Predicted liquid steel profile in slag and air region for single-plug configuration (**a**) side view and (**b**) top view; dual-plug configuration (**c**) side view and (**d**) top view.

## 4. Conclusions

In conclusion, the CFD predictions obtained from our study have addressed a request from the industry regarding the feasibility of incorporating a second plug into the existing plant configuration. The key findings can be summarized as follows:

1. Based on efficient single-phase modeling, the optimal position for the second plug is determined to be diametrically opposite to the existing plug at an equal radial distance. This configuration results in the lowest mixing time for a given total argon flow rate, indicating improved fluid dynamics within the ladle.
2. The variation in gas flow rates from the two plugs does not have a significant impact on mixing times as long as the total argon flow rate remains constant. However, an uneven distribution of argon leads to higher wall shear stresses. Therefore, it is recommended to maintain an equal flow rate distribution in the dual-plug configuration for effective argon purging.
3. The predicted results demonstrate reduced erosion on the uppermost part of the ladle's sidewall when utilizing the recommended two-plug position compared to a single-plug installation. The implementation of two plugs effectively lowers wall shear stresses, resulting in a reduced wear rate of the ladle refractory. This contributes to an extended service life of the refractory lining and a decrease in maintenance costs.
4. A dual-plug configuration offers the advantage of minimizing the oxidation of liquid steel. By utilizing two plugs, the surface area exposed to oxidation, known as the SOE

area, is significantly reduced. The reduction in the SOE area has a profound impact on maintaining the quality of the liquid steel by minimizing re-oxidation.

Based on these findings, it is recommended to incorporate a second plug in the proposed diametrically opposite position to the existing plug, with equal flow rate distribution, to optimize the ladle's mixing efficiency, reduce refractory erosion, and minimize steel re-oxidation. These insights provide valuable guidance for improving the plant configuration and enhancing the steelmaking process.

**Author Contributions:** Conceptualization: R.I.L.G., M.M.I., B.G. and C.L.; methodology: R.I.L.G. and M.M.I.; software: R.T. and R.I.L.G.; validation: R.T.; formal analysis: R.I.L.G., M.M.I., B.G., C.L. and R.T.; resources, R.I.L.G. and M.M.I.; writing of original draft preparation—R.T.; writing—review and editing: R.I.L.G. and M.M.I.; supervision, R.I.L.G. and M.M.I. All authors have read and agreed to the published version of the manuscript.

**Funding:** This research was funded by the NSERC and the CQRDA.

**Data Availability Statement:** The data presented in this study are available on request from the corresponding author. The data are not publicly available due to a confidentiality agreement with our industrial partner.

**Acknowledgments:** The authors acknowledge the financial support received from the Natural Sciences and Engineering Research Council of Canada (NSERC) and the Aluminum Research and Development Centre of Quebec (CQRDA), as well as member companies of the McGill Metals Processing Centre, for this work. The authors would also like to acknowledge the support in software licensing received from ANSYS Inc. to facilitate this research.

**Conflicts of Interest:** The authors declare no conflict of interest.

## References

1. Mazumdar, D.; Guthrie, R.I.L. Discussion on "Review of physical and numerical approaches for the study of gas stirring in ladle metallurgy". *Metall. Mater. Trans. B* **2020**, *51*, 412–416. [CrossRef]
2. Mazumdar, D.; Guthrie, R.I.L. The physical and mathematical modelling of gas stirred ladle systems. *ISIJ Int.* **1995**, *35*, 1–20. [CrossRef]
3. Liu, Y.; Ersson, M.; Liu, H.; Jonson, P.G.; Gan, Y. A review of physical and numerical approaches for the study of gas stirring in ladle metallurgy. *Metall. Mater. Trans. B* **2019**, *50*, 555–577. [CrossRef]
4. Joo, S.; Guthrie, R.I.L. Modeling flows and mixing in steelmaking ladles designed for single- and dual-plug bubbling operations. *Metall. Trans. B* **1992**, *23*, 765–778. [CrossRef]
5. Zhu, M.-Y.; Inomoto, T.; Sawada, I.; Hsiao, T.-C. Fluid flow and mixing phenomena in the ladle stirred by argon through multi-tuyere. *ISIJ Int.* **1995**, *35*, 472–479. [CrossRef]
6. Geng, D.-Q.; Lei, H.; He, J.-C. Optimization of mixing time in a ladle with dual plugs. *Int. J. Miner. Metall. Mater.* **2010**, *17*, 709–714. [CrossRef]
7. Liu, H.; Qi, Z.; Xu, M. Numerical simulation of fluid flow and interfacial behavior in three-phase argon-stirred ladles with one plug and dual plugs. *Steel Res. Int.* **2011**, *82*, 440–458. [CrossRef]
8. Villela-Aguilar, J.D.J.; Ramos-Banderas, J.A.; Hernández-Bocanegra, C.A.; Urióstegui-Hernández, A.; Solorio-Díaz, G. Optimization of the mixing time using asymmetrical arrays in both gas flow and injection positions in a dual-plug ladle. *ISIJ Int.* **2020**, *60*, 1172–1178. [CrossRef]
9. Tripathi, P.K.; Kumar, D.S.; Sarkar, A.; Vishwanath, S.C. Optimization of bath mixing and steel cleanliness during steel refining through physical and mathematical modeling. *Sādhanā* **2021**, *46*, 146. [CrossRef]
10. Jardón-Pérez, L.E.; González-Morales, D.R.; Trápaga, G.; González-Rivera, C.; Ramírez-Argáez, M.A. Effect of differentiated injection ratio, gas flow rate, and slag thickness on mixing time and open eye area in gas-stirred ladle assisted by physical modeling. *Metals* **2019**, *9*, 555. [CrossRef]
11. Chattopadhyay, K.; Sengupta, A.; Ajmani, S.K.; Lenka, S.N.; Singh, V. Optimization of dual purging location for better mixing in ladle: A water model study. *Ironmak. Steelmak.* **2009**, *36*, 537–542. [CrossRef]
12. Haiyan, T.; Xiaochen, G.; Guanghui, W.; Yong, W. Effect of gas blown modes on mixing phenomena in a bottom stirring ladle with dual plugs. *ISIJ Int.* **2016**, *56*, 2161–2170. [CrossRef]
13. Ramasetti, E.K.; Visuri, V.-V.; Sulasalmi, P.; Fabritius, T.; Savolainen, J.; Li, M.; Shao, L. Numerical modelling of the influence of argon flow rate and slag layer height on open-eye formation in a 150 ton steelmaking ladle. *Metals* **2019**, *9*, 1048. [CrossRef]
14. Mantripragada, V.T.; Sarkar, S. Slag eye formation in single and dual bottom purged industrial steelmaking ladles. *Can. Metall. Q.* **2020**, *59*, 159–168. [CrossRef]

15. Liu, W.; Tang, H.; Yang, S.; Wang, M.; Li, J.; Liu, Q.; Liu, J. Numerical simulation of slag eye formation and slag entrapment in a bottom-blown argon-stirred ladle. *Metall. Mater. Trans. B* **2018**, *49*, 2681–2691. [CrossRef]
16. Liu, Y.-H.; He, Z.; Pan, L.-P. Numerical investigations on the slag eye in steel ladles. *Adv. Mech. Eng.* **2014**, *2014*, 834103. [CrossRef]
17. Li, B.; Yin, H.; Zhou, C.Q.; Tsukihashi, F. Modeling of three-phase flows and behavior of slag/steel interface in an argon gas stirred ladle. *ISIJ Int.* **2008**, *48*, 1704–1711. [CrossRef]
18. Calderón-Hurtado, F.A.; Morales Dávila, R.; Chattopadhyay, K.; García-Hernández, S. Fluid flow turbulence in the proximities of the metal-slag interface in ladle stirring operations. *Metals* **2019**, *9*, 192. [CrossRef]
19. Singh, U.; Anapagaddi, R.; Mangal, S.; Padmanabhan, K.A.; Singh, A.K. Multiphase modeling of bottom-stirred ladle for prediction of slag–steel interface and estimation of desulfurization behavior. *Metall. Mater. Trans. B* **2016**, *47*, 1804–1816. [CrossRef]
20. Conejo, A.N.; Mishra, R.; Mazumdar, D. Effects of nozzle radial position, separation angle, and gas flow partitioning on the mixing, eye area, and wall shear stress in ladles fitted with dual plugs. *Metall. Mater. Trans. B* **2019**, *50*, 1490–1502. [CrossRef]
21. Llanos, C.A.; Garcia, S.; Ramos-Banderas, J.A.; Barreto, J.D.J.; Solorio, G. Multiphase modeling of the fluid dynamics of bottom argon bubbling during ladle operations. *ISIJ Int.* **2010**, *50*, 396–402. [CrossRef]
22. Sahai, Y.; Guthrie, R.I.L. Hydrodynamics of gas stirred melts: Part I. Gas/liquid coupling. *Metall. Trans. B* **1982**, *13*, 193–202. [CrossRef]
23. Goldschmit, M.B.; Owen, A.H.C. Numerical modelling of gas stirred ladles. *Ironmak. Steelmak.* **2001**, *28*, 337–341. [CrossRef]
24. Tiwari, R. Fluid Dynamic and Thermal Modeling of Homogeneous and Two-Phase Flows in a Ladle Shroud. Master's Thesis, Indian Institute of Technology, Kanpur, India, 2018.